

Structural Aspects of Microemulsions Using Dielectric Relaxation and Spin Label Techniques

V. K. BANSAL, K. CHINNASWAMY, C. RAMACHANDRAN, AND D. O. SHAH¹

Departments of Chemical Engineering, Anesthesiology and Biophysics, University of Florida, Gainesville, Florida 32611

Received December 4, 1978; accepted April 10, 1979

The structural characteristics of three similar systems containing sodium stearate, alcohol (*n*-pentanol, *n*-hexanol, or *n*-heptanol), hexadecane, and varying amounts of water were investigated. The systems were identical in composition except for the nature of alcohol used for producing microemulsions. In all the three microemulsion systems, the microemulsion remained isotropic and clear up to the water/oil ratio of 0.48. However, the electrical resistance studies indicated that the three systems were strikingly dissimilar. Upon increasing the water/oil ratio, *n*-pentanol microemulsion systems exhibited a constant decrease in resistance; hexanol microemulsion systems showed an initial increase and a subsequent sharp decrease whereas *n*-heptanol microemulsion systems exhibited very high electrical resistance which could not be measured ($>10^7 \Omega\text{-cm}$). The pentanol microemulsion systems exhibited dielectric relaxation at lower water/oil ratios as compared to the hexanol microemulsion systems. However, heptanol microemulsion systems did not exhibit dielectric relaxation. The dielectric relaxation results were interpreted in terms of ionization of the carboxyl group and the concomitant formation of the electrical double layer. This occurred at lower water/oil ratios in pentanol microemulsion systems as compared to hexanol microemulsion systems. However, there was no measurable ionization or electrical double layer formation in heptanol microemulsion systems. The spin label studies using a stearic acid spin probe suggested that the stearate molecule is located at the oil/water interface. Furthermore, the spin label incorporated in microemulsions exhibited anisotropic behavior in contrast to the isotropic behavior of the spin label dissolved in oil or water. The values of order parameter suggested that the order in interfacial film as measured by the spin label decreased in the following order: heptanol $>$ hexanol $>$ pentanol. In other words, the shorter chain alcohol produced a maximum disorder at the oil/water interface. The isotropic hyperfine splitting constant of the label in the three microemulsion systems suggested that the environment experienced by the spin label was intermediate between that of water and oil. In summary, the electric, dielectric, and ESR measurements suggest that the alcohol chain length affects the ionization, interfacial polarization, and disorder at the oil/water interface which in turn influences the properties of microemulsions.

INTRODUCTION

Ever since the introduction of microemulsions in the industry (1) and in the scientific world (2), they have received wide attention because of their applications in numerous fields of science and technology (3). The structure and properties of microemulsions were investigated by Schulman

and co-workers (4-7) who used various physical techniques such as light scattering, X-ray diffraction, electron microscopy, ultracentrifugation, electrical conductivity, and viscometry. From their observations they concluded that microemulsions are isotropic, clear or translucent, thermodynamically stable dispersions of oil, water, and emulsifiers with the droplet size ranging from 100 to 1000 Å in diameter.

Though "microemulsion" is the most widely used term for describing isotropic,

¹ Presently Visiting Professor of Chemical Engineering, Petroleum Engineering and the Institute for Energy Studies, Stanford University, Stanford, CA 94305.

clear, low viscosity dispersions of oil, water, and emulsifier, alternate terminology have been proposed by different workers (8–13).

Recently, Shah *et al.* (14) have reported the effect of alcohol chain length on the properties of potassium oleate–hexadecane microemulsions. Using various physical techniques such as birefringence, electrical resistance, high-resolution NMR (220 MHz), spin–spin relaxation time (T_2), and viscosity measurements, they have shown that *n*-hexanol and *n*-pentanol yield structurally dissimilar “microemulsion.” Shah and co-workers (15–19) have also shown that the microemulsion undergoes a series of structural changes as the amount of water is increased.

Dielectric properties of water-in-oil microemulsions have been reported by Clause *et al.* (20). They investigated the dielectric behavior of transparent water-in-hexadecane microemulsions using potassium oleate and *n*-hexanol as the emulsifier up to a critical mass fraction of water, $p_c = 0.32$ corresponding to clear to turbid transition. At the critical mass fraction of water, dielectric constant increased sharply due to interfacial polarization. They also observed a critical region of mass fraction from 0.20 to 0.32 where dielectric relaxation was prominent centering around 10 MHz. They referred to the microemulsions with water content below $p = 0.2$ as “hydrated micelles,” that between $p = 0.2$ or 0.32 as the “true microemulsions.” Eicke and Shepherd (21) observed a sudden increase in static dielectric constant as the amount of water solubilized in a system containing Aerosol AY increased. They have also studied the effects of electrolytes on the dielectric behavior of water-in-oil emulsion and they observed that the presence of electrolyte postpones the increase in dielectric increment to higher water/oil ratios.

Molecular motions in biological and model membranes have been investigated using ESR spin-labeling techniques (22–29). The properties of micellar solutions have also

been investigated using this technique (30–31). Recently, Menger *et al.* (32) and Kitahara *et al.* (33) used ESR spin labels to investigate the structural aspects of systems containing oil, surfactant, and water. Menger *et al.* (32) studied the effect of solubilized water in a di-2-ethylhexyl sodium sulfosuccinate–heptane system and correlated the splitting constant (A_N) with the “water pool” size in the system. It was observed that as the amount of water in the system increased the coupling constant also increased, indicating an increase in “water pool” size.

As can be seen from the literature, the ESR and dielectric studies have been carried out on several related systems. In order to obtain a better understanding of the structure of microemulsions, the above techniques along with electrical conductivity were used in the present study to investigate structural aspects of microemulsions containing sodium stearate, hexadecane, and various straight chain alcohols.

MATERIALS AND METHODS

Materials

Sodium stearate of 99% purity supplied by Matheson, Coleman and Bell Inc. was used for preparing microemulsions. All alcohols and oil were purchased from the Chemical Sample Company and were of greater than 99% purity. Triple distilled water was used in making all microemulsions.

Methods

Electrical resistance measurements. The electrical resistance of microemulsions was measured by a conductivity bridge (Beckman model RC 16B2). The electrical resistance of microemulsions having resistance greater than $10^6 \Omega$ was measured using a conductivity cell of cell constant 0.1 m^{-1} and microemulsion systems having lower resistance were measured using a conductivity cell of cell constant 1 cm^{-1} . The

water used in preparing the solutions had a specific conductance less than $1.0 \times 10^{-6} \Omega^{-1} \text{ cm}^{-1}$ in all measurements. All measurements were carried out at $25 \pm 0.1^\circ\text{C}$.

Dielectric constant measurements. The dielectric properties of the microemulsions were obtained using a "R-X Meter Type 250 B" (Boonton Radio Corporation—Division of Hewlett-Packard). The instrument is essentially a modified Schering bridge, to resolve the sample impedance into a resistance and capacitance in parallel. The frequency range of the instrument is 0.5–250 MHz and the resistance range is 14Ω to $100 \text{ M}\Omega$. The capacitance range of 0–20 pF can be increased to 0–120 pF by introducing calibrated inductors connected in parallel to the sample. Dielectric cells with variable electrode distances were designed similar to that of Sachs *et al.* (34) to operation in the frequency range of 0.5 to 150 MHz. The cells were made of cylindrical Teflon tubes with fixed stainless-steel electrodes fixed at the bottom. The movable electrode was shaped like a plunger kept in parallel to the bottom electrode by means of a Teflon collar. The pressure release holes facilitated a tight fit without any pressure buildup. In operation, the cell was screwed on vertically to the "hot" terminal while the movable electrode was connected to the "low" terminal which in turn was earthed. In tests with liquids of known dielectric constants the results were consistent with the literature data indicating the excellent operability of the cell.

The cell was filled with the sample using either a syringe or by just trickling down the sides ensuring that no air bubbles were trapped. Due to the very low voltage applied across the cell, there was no detectable rise in temperature. The dielectric measurements were made at selected frequencies (f) and at various electrode distances (l). The measured resistances (R_p) and capacitance (C_p) were the resolved components of the equivalent impedance ($Z = X - j2\pi f Y$) in parallel. X and Y were computed from the equivalent networks as

$$X = \frac{1/R_p}{(1/R_p)^2 + 4\pi^2 f^2 (C_p - C_1)^2}$$

$$Y = \frac{C_p - C_1}{(1/R_p)^2 + 4\pi^2 f^2 (C_p - C_1)^2}$$

where C_1 is the stray capacitance measured as the difference between the measured cell capacitance with air and the geometrical air condenser capacitance C_0 at various electrode distances. The sample capacitance and conductance vary inversely with l whereas polarization impedance is independent of l . It follows that X and Y vary linearly with l as

$$X = R_{tr} + \alpha l, \quad Y = -L_{tr} + \beta l$$

where R_{tr} and L_{tr} are the transmission line parameters. By means of linear least squares, the parameters α and β were estimated which could then be used to derive the dielectric parameters, namely

$$\text{Dielectric constant} \quad \epsilon' = \frac{C'_s}{C_0}$$

$$\text{Global dielectric loss factor} \quad \epsilon''_R = \frac{1}{2\pi f C_0 R'_s}$$

where

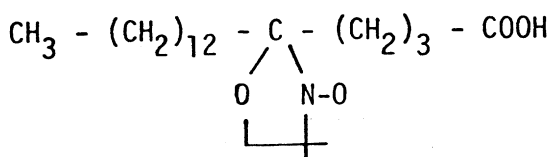
$$C'_s = \frac{\beta}{\alpha^2 + 4\pi^2 f^2 \beta^2}, \quad R'_s = \frac{\alpha^2 + 4\pi^2 f^2 \beta^2}{\alpha}$$

The dielectric loss factor ϵ'' was then computed by subtracting the conductance loss

factor measured at a low frequency from ϵ''_R . The electrode area was taken to be

the geometric area of the electrode itself and all the dielectric measurements were carried out at 27°C.

Electron spin resonance measurements. ESR measurements were carried out using a Varian E-9 spectrometer at a frequency of 9.5 GHz. The modulation amplitude employed was about 0.5 G and the time constant was 0.3 or 0.1 sec. All spectra were recorded at room temperature of $25 \pm 0.1^\circ\text{C}$ and each was the average of a minimum of two runs. Scan ranges were 100 and 40 G for order parameter determination and 4 G for line width measurements. The scan rate was about 2 G/min. The spin label used in the present study was obtained from Syva Company, Palo Alto, Calif., and was used as such. The structure of the label is shown below.



The concentration of spin label used was below $5 \times 10^{-4} M$ to avoid any exchange broadening.

Microemulsion Systems

Microemulsion systems were prepared using 1 g of sodium stearate, 4 ml of alcohol, and 10 ml of hexadecane; different amounts of water were added to make different W/O ratio microemulsions. The effect of emulsifier concentration on the properties of microemulsions was also studied by decreasing the amount of sodium stearate and hexanol to 0.5 g and 2 ml, respectively, and increasing the amount to 2 g and 8 ml keeping the volume of oil constant. Three alcohols (*n*-pentanol, *n*-hexanol, and *n*-heptanol) were used for studying the effect of alcohol chain length on microemulsion properties.

In our studies the microemulsions were prepared in two ways to check the pro-

cedural effects. In the first case a stock solution of the soap, oil, alcohol, and very little water was prepared to which water was added later. In the second method, a mixture of the required composition was directly prepared. The systems were found identical in their properties. It has to be mentioned that extreme care has to be taken to avoid bubble formation and entrapment of air during experimentation of dielectric and ESR properties. The systems studied were all very stable and remained isotropic over a long period of time. Their dielectric properties and electrical resistances remained the same. The systems returned to their original state after small perturbations in temperature.

RESULTS AND DISCUSSION

Figure 1 shows the effect of chain length of alcohols on the specific resistance of microemulsions (1 g of sodium stearate + 4 ml of alcohol + 10 ml of *n*-hexadecane) at different water/oil ratios. The upper part of Fig. 1 shows the behavior of the *n*-hexanol microemulsion system. The specific resistance increases as water/oil ratio is increased from 0.15 to 0.4 and then decreases sharply upon further addition of water up to a water/oil ratio of 0.48. After this the microemulsion turns translucent and separates into two phases on standing. The system reverts to a single phase at a water/oil ratio of 0.63, and is viscous and birefringent.

The lower curve in Fig. 1 indicates the electrical resistance of *n*-pentanol microemulsion system for various water/oil ratios. In contrast to *n*-hexanol microemulsion system, the specific resistance of *n*-pentanol microemulsion system decreased continuously for the water/oil ratios 0.15 to 0.48. The electrical resistance for *n*-heptanol microemulsion system was beyond the measuring range of the instrument ($2 \times 10^6 \Omega\text{-cm}$) for all water/oil ratios. It should be mentioned that all three microemulsion systems were isotropic and clear up to the water/oil ratio of 0.48.

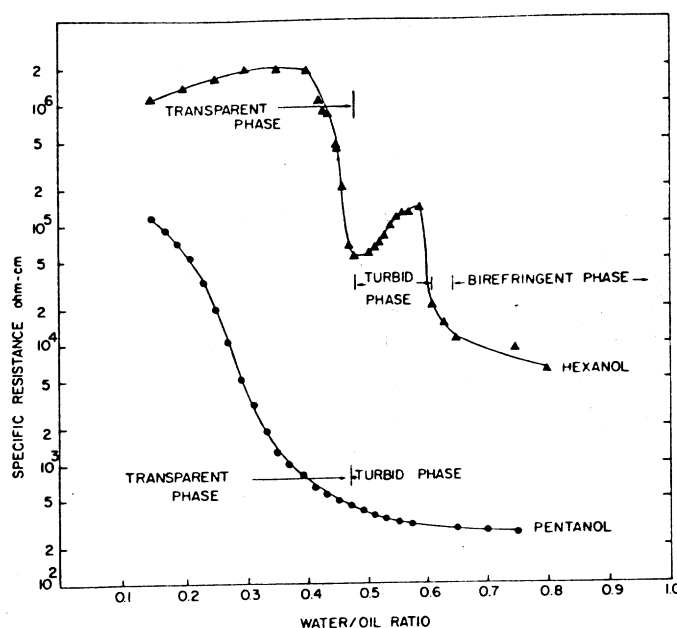


FIG. 1. Effect of alcohol chain length in electrical resistance of microemulsion at different water/oil ratio.

The results of dielectric behavior of microemulsions in the presence of various alcohols are shown in Fig. 2. The dielectric constant in *n*-pentanol increased monotonically up to the water/oil ratio of 0.3. Beyond this ratio the dielectric constant could not be measured due to very low electrical resistance (see Fig. 1). In the hexanol microemulsion system, the dielectric constant increased slowly up to the water/oil ratio of 0.4 beyond which a very sharp increment was observed. The heptanol microemulsion system did not show any appreciable change in dielectric constant up to the water/oil ratio of 0.5.

The dielectric relaxation behavior of these systems is shown in Figs. 3 and 4. It was observed that the pentanol microemulsion system exhibited a strong dielectric relaxation at low water contents (water/oil ratio ≈ 0.25) whereas the hexanol microemulsion system exhibited dielectric relaxation at higher water contents (water/oil ratio > 0.4). In the heptanol microemulsion system, the dielectric relaxation was not ob-

served even at high water contents (water/oil ratio ≈ 0.5). It should be noted that the critical frequency of relaxation decreases with an increase in the water/oil ratio (Figs. 3 and 4). This suggests that the thickness or the radius of the ionic atmosphere increases provided the surface conductance model of Schwarz (35) is applicable to these systems. A similar observation and conclusion was made by Sachs *et al.* (36) for polyelectrolyte solutions.

In Fig. 5 the effect of the concentration of emulsifiers (sodium stearate and *n*-hexanol) on the specific resistance is shown. As can be seen from the results, the general trend is the same for all emulsifier concentrations. The decrease in the electrical resistance occurred at a higher water/oil ratio as the emulsifier concentration was increased. The isotropic clear region and hence the water solubilization capacity increased with emulsifier concentration. The dielectric behavior of all the systems was quite similar. The critical water/oil ratio (water/oil ratio at which the asymp-

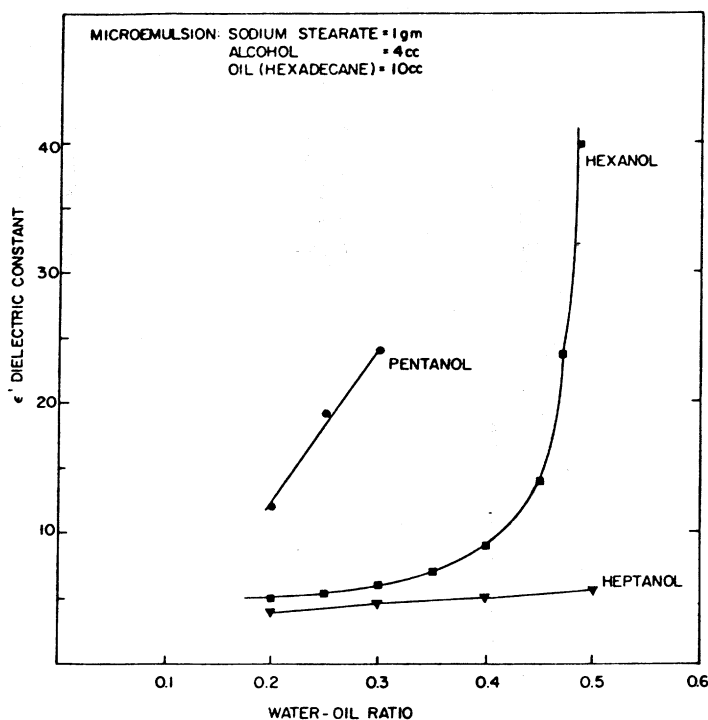


FIG. 2. Effect of alcohol chain length on dielectric constant of microemulsion at 2MHz frequency.

otic increase in dielectric constant occurs) increased with emulsifier concentration (Fig. 6).

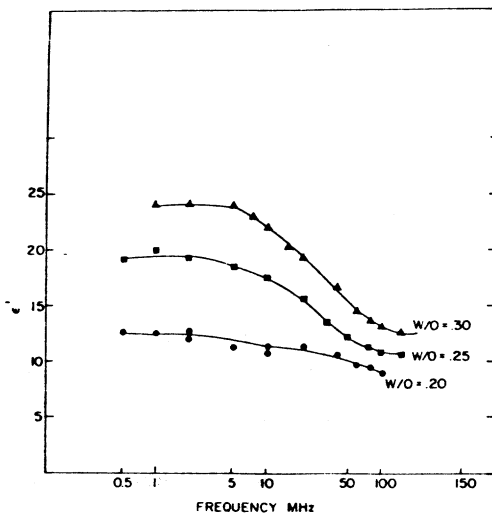


FIG. 3. Effect of water/oil ratio on dielectric constant (ϵ') of pentanol-stearate-hexadecane microemulsion.

Figure 7 shows the critical water/oil ratio (V_c) at different emulsifier concentrations. The plot of V_c versus emulsifier concentration gives a straight line. The slope of the line gives the number of water molecules per molecule of soap at the critical ratio where the microemulsion is about to break down. The ratio comes out to be 115 molecules of water per molecule of soap. Based on this number, if one calculates the amount of surfactant at the interface of the droplets at the critical water/oil ratio of 0.485 (i.e., 4.85 ml water, 4 ml *n*-hexanol, 10 ml hexadecane, and 1 g sodium stearate), it turns out that only ~ 0.717 g of sodium stearate is at the oil/water interface. This leads to the conclusion that all surfactant molecules are not at the oil/water interface and a fraction presumably dissolves in the oil and/or water phase. It should be noted that several investigators have assumed that all surfactant or soap molecules are located at the oil/water interface in microemulsions.

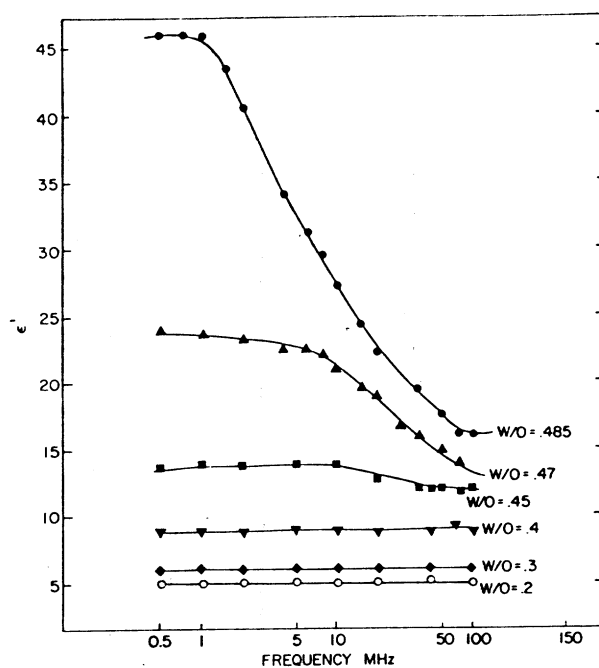


FIG. 4. Effect of water/oil ratio on dielectric constant (ϵ') of hexanol-stearate-hexadecane microemulsion.

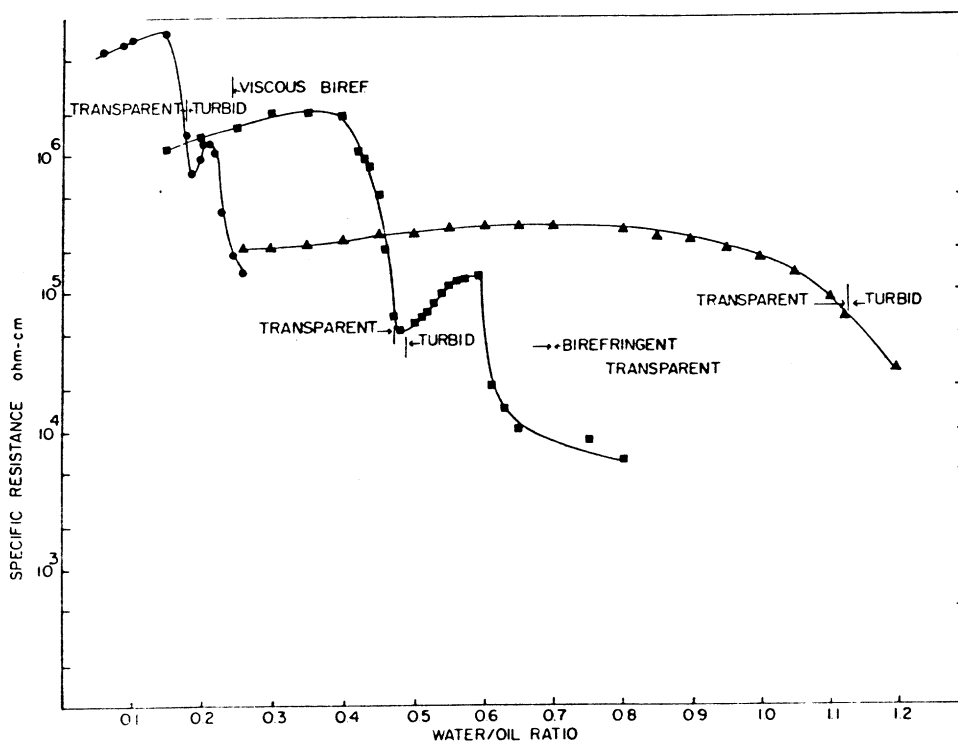


FIG. 5. Effect of emulsifier concentration on electrical resistance of microemulsion at different water/oil ratio.

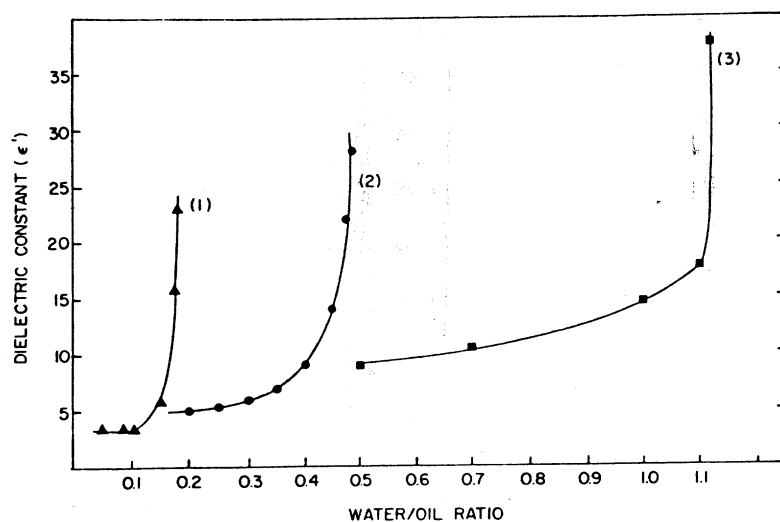


FIG. 6. Effect of emulsifier concentration on dielectric constant ϵ' of microemulsion at 2MHz frequency.

Figure 8A shows the ESR spectrum of the spin-labeled fatty acid in hexadecane oil. Such three line spectra are obtained whenever the fatty acid chain is not anchored strongly at the oil/water interface via the carboxylate group. Figure 8B shows the spectrum of the spin-labeled stearic acid in the hexanol microemulsion system. It is

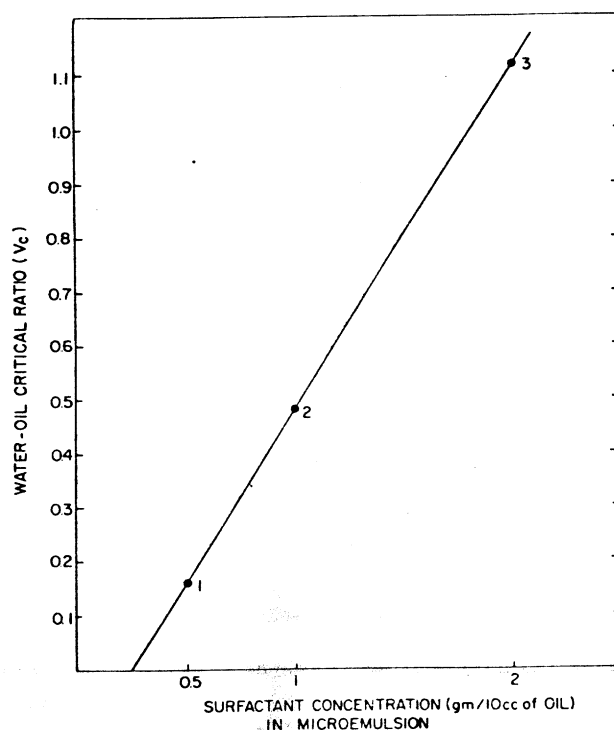


FIG. 7. Critical ratio V_c for microemulsions at different emulsifier concentration in microemulsion system.

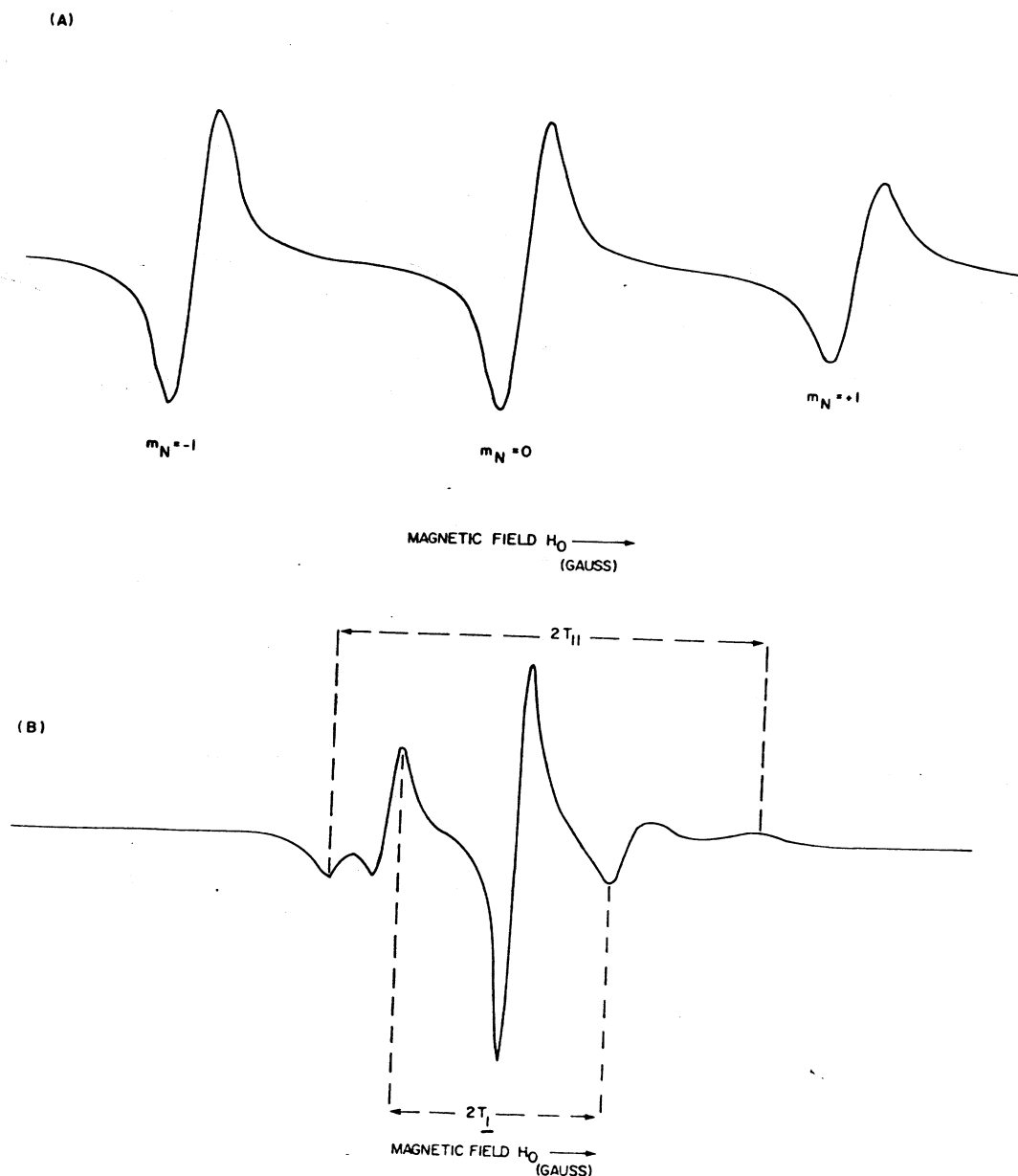


FIG. 8. ESR Spectra of 5-doxyl stearic acid in hexadecane and microemulsion. (A) ESR spectrum of $5.0 \times 10^{-4} M$ 5-doxyl stearic acid in hexadecane; (B) ESR spectrum of $5.0 \times 10^{-4} M$ 5-doxyl stearic acid in sodium stearate/hexanol/hexadecane microemulsion at water/oil ratio of 0.3.

immediately noticed that the spectrum has fairly well-defined extrema. This spectrum is anisotropic in nature. Similar spectra have been obtained for spin-labeled phospholipid dispersions (22), egg lecithin vesicles (23), and normal sarcoplasmic

vesicles (24), for stearic acid labels. The observed shape of such spectra has been identified with that arising from axial symmetry of nitroxide group motional characteristics. This situation arises mainly due to a strong anchoring of the fatty acid

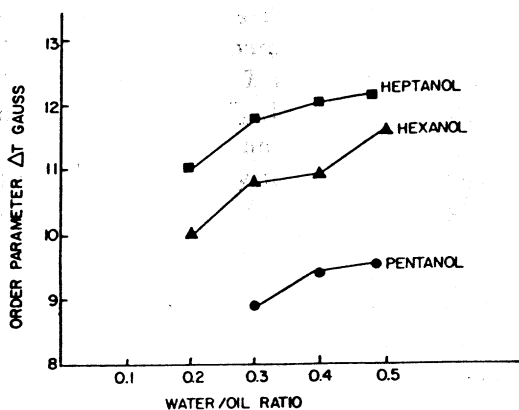


FIG. 9. Effect of alcohol chain length on order parameter (ΔT) in sodium stearate microemulsion at different water/oil ratios.

chain through the carboxyl group at the oil/water interface. Before we discuss the spin-labeling data, it is appropriate to mention a few characteristics of spin-labeled fatty acid motion in dispersions. The theory associated with the motion of fatty acid labels in membranes, vesicles, and dispersions is well documented (22–30). There are two types of molecular motion that the nitroxide group of the spin-labeled fatty acid can undergo. Each carbon–carbon segment of the fatty acid chain can have independent motion, termed flexing mobility, and in saturated chains this mobility is known to be high. As the nitroxide group is moved toward the carboxyl group, the mobility decreases indicating a more rigid state of the chain near the interface (25). A second type of molecular motion for the nitroxide moiety is a rotation about the long molecular or chain axis. The spin probe long axis precesses rapidly around the normal to the interface and describes a cone. The $2p\pi$ orbital of the nitrogen of the nitroxide group makes an angle β with the normal and this angle denotes the deviation from normal. An increase in β indicates a less ordered fatty acid chain. The rapid anisotropic motion about the molecular axis imparts axial symmetry giving rise to two modes of interaction between the spin and

the external magnetic field. The observed splittings with the applied field parallel to the axis of rotation is denoted by T_{\parallel} and that in the perpendicular direction T_{\perp} (Fig. 8B). The quantity $T_{\parallel} - T_{\perp}$, ΔT , is an indirect measure of the order in the system. The order parameter S is given by

$$S = (T_{\parallel} - T_{\perp}) / (T_{zz} - T_{xx}),$$

where T_{zz} and T_{xx} are the splittings when the spin label is oriented parallel and perpendicular, respectively, to the magnetic field. The values for T_{zz} and T_{xx} obtained for the spin label used here were taken from the literature (27). The order parameter S is related to the angle of deviation, β , through the expression

$$S = (1/2) \times (3 \cos^2 \beta - 1).$$

Therefore, a decrease in order parameter, S , denotes an increase in deviation of the rotational axis from the normal. An increase in angle of deviation β is an indication of increased mobility of the chains.

It is seen therefore that fatty acid labels undergo fast anisotropic motion about the molecular axis in addition to a flexing motion. Spectra with a high degree of anisotropy and well-defined extrema are obtained (Fig. 8B). If the amplitude of motion of the spin label is increased and coupled with a decrease in the rate of rotation, the anisotropy disappears and isotropic three line spectra are obtained. The flexing motion of the chains in these cases is enhanced making the chains more mobile.

ESR order parameters ΔT for the three alcohol systems are shown in Fig. 9. ΔT increases upon addition of water in all three systems. The relative magnitudes are in the order pentanol < hexanol < heptanol. This indicates that the structural organization is least rigid in pentanol followed by hexanol and heptanol. Addition of water enhances the order of the fatty acid chains near the polar group region, especially at the fifth carbon position where the spin label was attached. The variation of the hyper-

fine splitting constant A_N of the label upon addition of water in the three systems is shown in Fig. 10. A_N can be calculated from the experimental values of $T_{||}$ and T_{\perp} through the expression (24),

$$A_N = (T_{||} + 2T_{\perp})/3,$$

where A_N reflects the polarity of the label environment. It is observed that in all three systems, the values of A_N lie between those obtained in water (15.6 G) and in hexadecane (13.1 G). This indicates that the addition of water affects the polarity of the label at the fifth carbon position. The increasing trend in A_N values reflects an increase in water pool size (32). The variation of linewidth of central line, W_0 , for the three systems is summarized in Table I. The linewidths in all three systems are comparable in magnitude and show a decreasing trend upon addition of water. Similar trends have been reported by Menger *et al.* (32) and corroborates the view that increasing water pool size increases A_N and decreases linewidth. The reduction in linewidth is also consistent with an increase in rotational frequency of the nitroxide ring about the long chain axis as evidenced by an increase in anisotropy

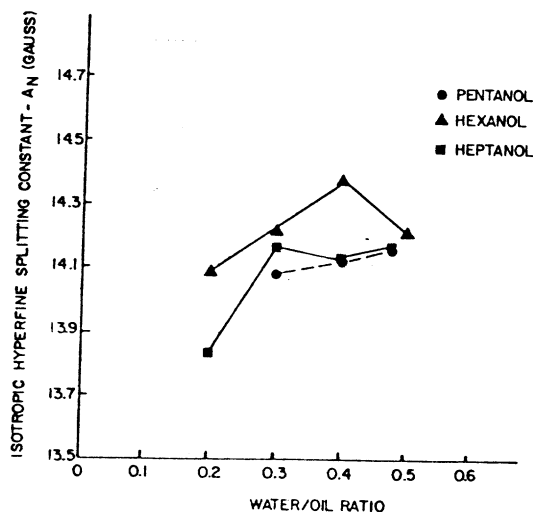


FIG. 10. Effect of alcohol chain length on hyperfine splitting constant (A_N) of 5-doxyl stearate in sodium stearate microemulsions at different water/oil ratios.

Journal of Colloid and Interface Science, Vol. 72, No. 3, December 1979

TABLE I

Effect of Alcohol Chain Length on Linewidth of Central Line of 5-Keto Stearic Acid in Sodium Stearate Microemulsions at Different Water/Oil Ratios

Water/oil ratio	Linewidth, W_0 (G)		
	Pentanol	Hexanol	Heptanol
0.20	1.94	2.0	2.02
0.30	1.94	1.98	1.96
0.40	1.90	1.98	1.92
0.48	1.90	1.93	1.88

and order parameter ΔT follows the trend, pentanol < hexanol < heptanol. The angle of deviation β from normal therefore increases in the order pentanol > hexanol > heptanol (Table II).

The above two results suggest that the nitroxide group of the label has a reduced rotational frequency about the long chain axis and that the chains themselves have an increased amplitude of motion in pentanol microemulsion systems. These observations indicate that the probability of a stearic acid label encountering a surfactant or alcohol molecule is higher in pentanol microemulsion systems, as compared to hexanol or heptanol microemulsion systems.

From electric, dielectric, and spin-label results, a model for the interfacial structure of microemulsions in the presence of *n*-pentanol, *n*-hexanol, or *n*-heptanol can be proposed as follows. If we consider that the water droplets in microemulsions are stabilized by a mixed film of soap and alcohol, the number of alcohol molecules

TABLE II

Effect of Alcohol Chain Length on Angle of Deviation for 5-Keto Stearic Acid Label in Sodium Stearate Microemulsions at Different Water/Oil Ratios

Water/oil ratio	Angle of deviation, β (degrees)		
	Pentanol	Hexanol	Heptanol
0.3	35.01	30.52	28.00
0.4	34.00	30.20	27.30
0.5	33.55	28.3	27.00

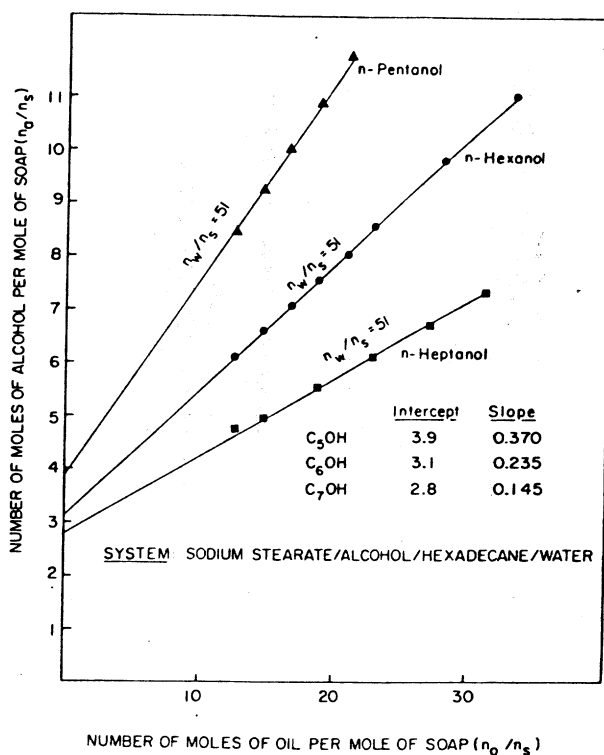


FIG. 11. Effect of alcohol chain length in formation of microemulsions.

per soap molecule would depend upon the partitioning of alcohol between oil, interface, and aqueous phase. The partitioning of alcohol between the different phases would depend upon the nature of surfactant, chain length of oil and alcohol, and the ionic strength of the aqueous phase. Thus, the number of alcohol molecules per soap molecule at the interface should decrease as the chain length of alcohol increases. The higher-chain length alcohol would preferentially partition into the oil phase as compared to the interface or water. Accordingly, more pentanol molecules per soap molecule would be at the interface and hence more disorder would be produced in the alkyl chain of the soap molecules. The spin-label results corroborate this interpretation. This model also provides an explanation of the dielectric behavior of these microemulsions. In the pentanol microemulsion system, the average intermolecular

distance between soap molecules would be greater as compared to hexanol or heptanol microemulsion systems upon addition of water. This is in agreement with the observed dielectric relaxation (or interfacial polarization) of these microemulsions.

The above mentioned hypothesis (i.e., more pentanol per soap molecule at the oil/water interface as compared to hexanol or heptanol) was confirmed by alcohol/oil titration results shown in Fig. 11. This approach was used by Bowcott and Schulman (37) to determine the alcohol/soap ratio at the interface and to determine the critical alcohol/oil ratio necessary to form microemulsions. According to this model (37), the intercept on y axis represents the molar ratio of alcohol to soap at the interface and the slope of each plot represents the critical molar ratio of alcohol/oil necessary to produce microemulsions. As can be seen from Fig. 11, the alcohol/soap ratio at the

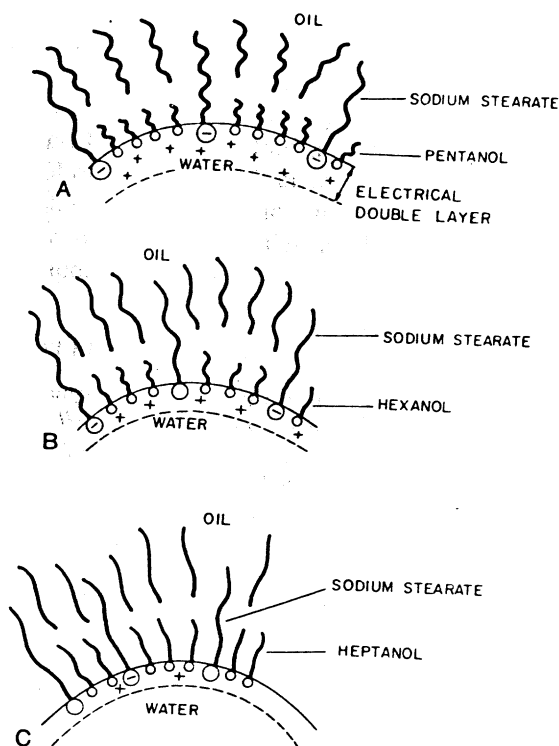


FIG. 12. Schematic presentation of the effect of alcohol chain length on molecular motion, interfacial composition of surfactant and alcohol, and the thickness of electrical double layer. A, B, C illustrate respectively that an increase in the alcohol chain length decreases the molar ratio of alcohol to soap at the interface, intermolecular spacing and the degree of ionization of carboxyl groups, the thickness of electrical double layer and the disorder of alkyl chains at the interface.

interface is 3.9, 3.1, and 2.8 for pentanol, hexanol, and heptanol microemulsion systems, respectively. Hence, we have shown in this study that a higher alcohol/soap ratio at the interface for pentanol as compared to hexanol or heptanol leads to greater disorder as observed with the spin label and to early ionization of soap as shown by electrical resistance and dielectric relaxation.

Figure 12 illustrates schematically the conclusions based on the spin-label, electrical, dielectric, and titration studies. The disorder of molecules at the interface, the surfactant-alcohol ratio at the interface, and the change in the thickness of electri-

cal double layer inferred from the above-mentioned measurements for each alcohol system are shown in Fig. 12. In summary, the results presented here indicate that the chain length of alcohol strikingly influences the order (i.e., the flexibility) and the ionization behavior of soap molecules at the oil/water interface.

ACKNOWLEDGMENTS

This work has been supported by the Department of Energy, Grant No. EW-78-S-19-0008, and a consortium of 20 major oil and chemical companies for the Improved Oil Recovery Research Program at the University of Florida.

REFERENCES

1. Kokatnur, V. R., U. S. Patent 2,111,100 (1935).
2. Hoar, T. P., and Schulman, J. H., *Nature (London)* **152**, 102 (1943).
3. Prince, L. M., in "Microemulsions, Theory and Practice," Academic Press, 1978.
4. Schulman, J. H., and Riley, D. P., *J. Colloid Sci.* **3**, 383 (1948).
5. Schulman, J. H., and Friend, J. A., *J. Colloid Sci.* **4**, 497 (1949).
6. Schulman, J. H., Stoeckenius, W., and Prince, L. M., *J. Phys. Chem.* **63**, 1677 (1959).
7. Stoeckenius, W., Schulman, J. H., and Prince, L. M., *Kolloid-Z.* **169**, 170 (1960).
8. Gerbacia, W., and Rosano, H. L., *J. Colloid Interface Sci.* **44**, 242 (1973).
9. Adamson, A. W., *J. Colloid Interface Sci.* **29**, 261 (1969).
10. Shinoda, K., and Kunieda, H., *J. Colloid Interface Sci.* **42**, 381 (1973).
11. Gillberg, G., Lehtinen, H., and Friberg, S., *J. Colloid Interface Sci.* **33**, 40 (1970).
12. Sjöblom, E., and Friberg, S., *J. Colloid Interface Sci.* **67**, 16 (1978).
13. Friberg, S., and Buraszczenka, I., *Prog. Colloid Polym. Sci.* **63**, 1 (1978).
14. Shah, D. O., Walker, R. D., Jr., Hsieh, W. C., Shah, N. J., Dwivedi, S., Nelander, J., Pepinsky, R., and Deamer, D. W., SPE 5815, presented at Improved Oil Recovery Symposium of SPE of AIME, Tulsa, Oklahoma, March 22-24, 1976.
15. Shah, D. O., and Hamlin, R. M., Jr., *Science* **171**, 483 (1971).
16. Shah, D. O., Tamjeedi, A., Falco, J. W., and Walker, R. D., Jr., *AIChE J.* **18**, 1116 (1972).
17. Falco, J. W., Walker, R. D., Jr., and Shah, D. O., *AIChE J.* **20**, 510 (1974).

18. Shah, D. O., Bansal, V. K., Chan, K. S., and Hsieh, W. C., in "Improved Oil Recovery by Surfactant and Polymer Flooding" (D. O. Shah and R. S. Schechter, Eds.), p. 293. Academic Press, New York, 1977.
19. Shah, D. O., *Ann. N. Y. Acad. Sci.* **204**, 125 (1973).
20. Claussé, M., Sheppard, R. J., Boned, C., and Essex, C. G., in "Colloid Interface Science" (M. Kerker, Ed.), Vol. II, p. 353. Academic Press, New York, 1976.
21. Eicke, H. F., and Shepherd, C. J. W., *Helvet. Chim. Acta* **57**, 1951 (1974).
22. McConnell, H. M., and McFarland, B. G., *Quart. Rev. Biophys.* **3**, 91 (1970).
23. Schreier-Muccillo, S., Marsh, D., Dugas, H., Schneider, H., and Smith, I. C. P., *Chem. Phys. Lipids* **10**, 11 (1973).
24. Seelig, J., and Hasselbach, W., *Eur. J. Biochem.* **21**, 17 (1971).
25. Hubbell, W. L., and McConnell, H. M., *J. Amer. Chem. Soc.* **93**, 314 (1971).
26. Smith, I. C. P., in "Biological Applications of Electron Spin Resonance Spectroscopy" (J. R. Bolton, D. Borg, and H. Schwarz, Eds.), p. 483. Wiley-Interscience, New York, 1972.
27. Seelig, J., *J. Amer. Chem. Soc.* **92**, 3881 (1970).
28. Sanson, A., Ptak, M., Rigaud, J. L., and Gary-Bobo, C. M., *Chem. Phys. Lipids* **17**, 435 (1976).
29. Shiga, T., Suda, T., and Maeda, N., *Biochim. Biophys. Acta* **466**, 231 (1977).
30. Ernandes, J. R., Chaimovich, H., and Schreier, S., *Chem. Phys. Lipids* **18**, 304 (1977).
31. Atherton, N. M., and Starch, S., *J. Chem. Soc. Faraday Trans. II* **68**, 374 (1972).
32. Menger, F. M., Saito, G., Sanzero, G. V., and Dodd, J. R., *J. Amer. Chem. Soc.* **97**, 909 (1975).
33. Kitahara, A., Ohashi, O., and Kon-no, K., *J. Colloid Interface Sci.* **49**, 108 (1974).
34. Sachs, S. B., Katchalsky, A., and Spiegler, K. S., *Electrochim. Acta* **15**, 693 (1970).
35. Schwarz, G., *J. Phys. Chem.* **66**, 2636 (1962).
36. Sachs, S. B., Raziell, A., Eisenberg, H., and Katchalsky, A., *Trans. Faraday Soc.* **65**, 577 (1969).
37. Bowcott, J. E., and Schulman, J. H., *Z. Electrochem. Phys. Chem.* **59**, 283 (1955).